LASER INTERFEROMETER GRAVITATIONAL WAVE OBSERVATORY

LIGO Laboratory / LIGO Scientific Collaboration

LIGO- T0900435-v9 *LIGO* 10th September 2013

HAM Small Triple Suspension Final Design Document

Norna A Robertson, Mark Barton, Mike Meyer, Janeen Romie, Calum Torrie, Jeff Kissel

Distribution of this document:
LIGO Scientific Collaboration

This is an internal working note
of the LIGO Laboratory.

California Institute of Technology
LIGO Project – MS 18-34
1200 E. California Blvd.
Pasadena, CA 91125
Phone (626) 395-2129
Fax (626) 304-9834
E-mail: info@ligo.caltech.edu

Massachusetts Institute of Technology
LIGO Project – NW22-295
185 Albany St
Cambridge, MA 02139
Phone (617) 253-4824
Fax (617) 253-7014
E-mail: info@ligo.mit.edu

LIGO Hanford Observatory
P.O. Box 1970
Richland WA 99352
Phone 509-372-8106
Fax 509-372-8137

LIGO Livingston Observatory
P.O. Box 940
Livingston, LA 70754
Phone 225-686-3100
Fax 225-686-7189

http://www.ligo.caltech.edu/

v2 - revised with various additions following requests from Final Design Review committee members, including: new section (5) on OSEMS, Magnets and DC control ranges, reference to document T0900588 incorporating modal shapes, information (fig 2) on provision of holes in structure for various applications, clarification on baseline choice for suspension wire radius (4.4), information on gluing prisms (4.5), attaching magnets (4.6), and adjusting suspension for variation in masses (4.7), information on seismic input (11.4) and damping control law (11.5) used for producing noise curves
v3 – includes value of roll lever arm in section 5.v4 – Table showing details of OSEMS, Magnets and DC Control Ranges (section 5) has been updated, Jan 30 2013.
v5 – added link info to actuator noise estimates (section 6), updated Section 7 (RODAs etc) including a new section on further design reviews. v6 – added another RODA. v7 - updated section 7 re ECR E1201116 –actions completed. v8 – added another RODA. v9 – added another RODA

Contents

Section 1: Introduction

Section 2: Requirements

Section 3: Resolution of action items from PDR

Section 4: Mechanical Design

Section 5: OSEMs, Magnets and DC Control Ranges

Section 6: Noise Estimates

Section 7: Final Design Review Checklist

Section 8: Conclusions

Section 9: Details of MATLAB model

Section 10: Details of Mathematica model

Section 11: Appendices

1 Introduction

The purpose of this document is to describe the final design of the HAM Small Triple Suspension (HSTS). The HSTS will be used for the input modecleaner optics IMC1, 2, 3 and the small optics within the recycling cavities, PRM, PR2, SRM and SR2. The HSTS, was formerly called the Input Modecleaner Suspension, since the suspension design was originally intended only for the input modecleaner mirrors which have dimensions 150 mm diameter by 75 mm thick. When the decision was taken in spring of 2008 to move to a stable recycling cavity configuration, it was recognised that the same suspension design could be used for the small optics within each recycling cavity. The current requirements for the suspensions for each type of optic are given in section 2. Responses to action items from the PDR are in section 3. The mechanical design is discussed in section 4, including changes and revisions since the PDR. Information on OSEMs and magnets and DC control ranges is given in section 5. Suspension thermal noise and seismic noise estimates are discussed in section 6. The final design review checklist is discussed in Section7. Section 8 gives conclusions. Sections 9 and 10 give information on the MATLAB and Mathematica models respectively. Section 11 consists of appendices covering diagrams and nomenclature details of the parameters of a triple pendulum, further information on the Mathematica model, and information on input used to derive noise curves.

This document supersedes the preliminary design document T080187-00. That document gave extensive information on the history of the design and requirements for this suspension and on the work done on prototypes. That information is not repeated here.

2 Requirements

The current requirements for displacement noise for the recycling cavities are laid out in the document “Displacement Noise in Advanced LIGO Triple Suspensions”, M Evans and P Fritschel (T080192-01-D), and formally given in the Cavity Optic Design Requirements Document T010007-v2. The total displacement noise for the signal recycling cavity length (SCRL) is given in figure 2 of T080192. The requirement has a value at 10 Hz of 3×10^{-17} m/√ Hz falling to 2×10^{-18}

m/√ Hz at 30 Hz and then flattening off. The slope from 10 to 30 Hz goes as $f^{-2.5}$. This is the *total noise* suitably summed over all the recycling cavity optics. We can make some assumptions to arrive at an approximate requirement for each optic, noting that in practice the small and large triples are similar (though not identical) in their transfer functions and suspension thermal noise estimates. From T080192, the total SRCL noise is calculated according to

$$x_{SRCL} = (x^2_{HSTS} + (2x_{HSTS})^2 + (2x_{HLTS})^2)^{1/2}. \quad \text{Eqn 1}$$

Assume that $x_{HSTS} = x_{HLTS}$. Thus the requirement for x_{HSTS} at 10 Hz is given by $(3 \times 10^{-17})/(\sqrt{9}) = 1 \times 10^{-17}$ m/√ Hz, and at 30 Hz is given by $2 \times 10^{-18}/(\sqrt{9}) = 6.7 \times 10^{-19}$ m/√ Hz. As we will see later, this value is close to the expected suspension thermal noise limit for this suspension on steel wires, making certain assumptions about the material loss and clamp design. Also the slope is the expected thermal noise slope. Thus we can meet this noise limit if residual seismic noise lies below the expected thermal noise.

We note that the requirements imposed on these suspensions are set to achieve a signal recycling cavity length noise which lies at least a factor of 10 below the aimed-for differential arm displacement noise for the interferometer, so that slightly exceeding these requirements does not immediately impact the interferometer sensitivity.

In addition to these formal requirements, there are several recommendations in T080192 which we were asked to consider. We repeat these below.

- The suspension thermal noise level is acceptable, provided the effective wire loss is close to $2x10^{-4}$, so care needs to be taken in the implementation to achieve this.
- Efforts should be made to increase the vertical seismic isolation, particularly in the 10-20 Hz band.
- Consideration should be given to making the highest vertical eigenfrequency (the `bounce mode') the same for both small and large triples (probably the higher frequency of the current small triple design is preferred).

The requirements for the suspension as used in the input modecleaner cavity are relaxed from those given above. For each suspension the total noise should not exceed $3x10^{-15}$ m/√ Hz at 10 Hz falling to $2x10^{-17}$ m/√ Hz at 100 Hz (see T010007-v2).

In addition to the noise requirements, we have a requirement to adapt this suspension to take two different types of optics. The input modecleaner optics and the small recycling mirror optics, although nominally the same, in fact differ in wedge angle (and hence mass) and in orientation. The mass difference and how we allow for this in the suspension design is further discussed in section 4. The details of these parameters have changed since the preliminary design review for the HSTS. The current details as supplied by the IO group are captured in E0900342.

3 Resolution of action items from PDR

The report from the PDR is M0900018-v1. Points raised in the report and the actions taken are as follows.

3.1 Electronics

As noted on page 2 of the report, the triple electronics were not ready for review at the time of the PDR for the HSTS and HLTS. Under “Action items”, we were asked to prepare a schedule and carry out preparations for an Electronics PDR. After extensive discussions, it was agreed that the US team would took over the detailed design and prototyping of the analogue part of the triple electronics, building on the work already undertaken in the UK, to help the UK meet production schedules by accelerating the prototyping phase. This work has been carried out and subsequently reviewed at an FDR level by a team led by Vern Sandberg, and final review reports have now been issued. It has been agreed that the final design review of the US part of the electronics and the integration of the US and UK parts will take place when the HAM large triple suspension (HLTS) final design review is held (currently scheduled for February` 2010). Full details of the electronics will be given at that time. We include in this document the current requirements and DC control ranges for the HSTS, along with details of the usage of OSEMS and magnets. See section 5.

3.2 28 Hz vertical peak and vertical isolation

No specific recommendations on an approach to these issues were given. We were asked to consider two paths

3.2.1 The use of higher strength maraging blades to lower vertical frequencies and hence increase isolation.

We have considered this and concluded that there is no strong advantage to using higher strength material. This is captured in RODA M0900234-v1 “SUS (US) blades will use maraging 250” The following statement appears in the RODA “Given that the creep rate of maraging 250 has been demonstrated to be low, and that only a modest increase in isolation would result from using 300, we advocate using maraging 250 in all Advanced LIGO suspensions.” Further details can be found in the RODA.

3.2.2 Determine with the SEI team if modeling indicates coupling to SEI of the 28 Hz peak and if this might present a problem.

We have been in contact with Fabrice Matichard regarding this suggestion, noting that if such coupling existed it should be seen at LASTI between the quad suspension (highest vertical mode at ~17 Hz) and the BSC-ISI, and asking if there was any evidence for this. In his reply Fabrice commented that there is nothing noticeable at 17 Hz on the BSC-ISI and in his opinion it would be more useful to spend time testing rather than modeling. Further testing may be possible when a HAM-ISI is installed at LASTI, and either an HSTS or an HLTS prototype could be put on it. Lacking any current experimental evidence that there might be a problem with the 28 Hz peak, we are not advocating any radical change to the design. We consider the use of thinner wire to push this frequency lower in section 4.3.

3.3 Maximum acceptable weight

We were asked to coordinate with SYS on the maximum acceptable weight for the HSTS and HLTS suspensions based on recent layout information. We are in close collaboration with SYS on this issue and will continue to liaise with them. At present it looks like we will be saving some weight with the HSTS (number currently in use by SYS in their budget = 72.5 kg and number for updated HSTS design = 65.1 kg excluding any trim mass needed during assembly).

4 Mechanical Design

4.1 Overall suspension design

The basic design for this suspension is based on the GEO triple pendulums (see T010103), with two key differences which are simplifications.

i) steel wires instead of silica fibres in the final stage

ii) no triple reaction pendulum for applying global control. See T020059-01-D for justification of removal of the reaction pendulum.

The key design features are as follows

- Triple pendulum with three masses of approximately equal mass and approximately equal lengths.*
- Two stages of cantilever springs made of maraging steel blades for good vertical isolation: top stage consists of two blades from which two wires go down to the top mass, and lower stage consists of four blades within the top mass with four wires going down to the intermediate mass.
- Damping of all of the low frequency modes of the triple pendulum uses 6 co-located sensors and actuators at the top mass of the triple pendulum. To achieve adequate damping the design has to be such that all the modes couple well to motion of the top mass.
- DC alignment of optic yaw and pitch is done by applying forces to the actuators at the highest mass. This requires that the intermediate mass and the optic are each suspended by four wires, two on each side, so that the system behaves like a marionette from the top mass downwards.
- Global control forces can be applied at the intermediate mass and the optic in a hierarchical manner using electromagnetic forces, with the magnets attached to the back of the masses and the coils attached to the support structure.

*The choice of equal masses and equal wire lengths as a baseline has come from experience with previous designs and leads to good coupling of modes. In addition using three equal lengths gives the best isolation for a given overall length.

The suspension has to fit within the HAM chambers. This limits the overall length of the suspension within its support structure. Currently the length from top blade to centre of optic for the small triple is approximately 0.69 m. The size of the optic (ignoring wedge) is 150 mm diam x 75 mm thick, and mass ~ 3 kg.

The detailed set of mechanical parameters, as used in the MATLAB model with values as of October 2009, is given in Section 9. The listing includes the expected normal mode frequencies for the suspension. A set of modal shapes, derived using Mark Barton's Mathematica model of the suspension can be found at T0900588.

Diagrams and notes explaining the key nomenclature used for the triple suspension parameters are given in Section 11.1 and 11.2.

Detailed engineering drawings can be found from links on the review wiki page.

Fig 1 shows a Solidworks rendering of the final design, with a dummy metal mass in place of the mirror. The purple beams indicate the laser beam reflecting from the optic and are used to check that there is no obscuration by earthquake stops.

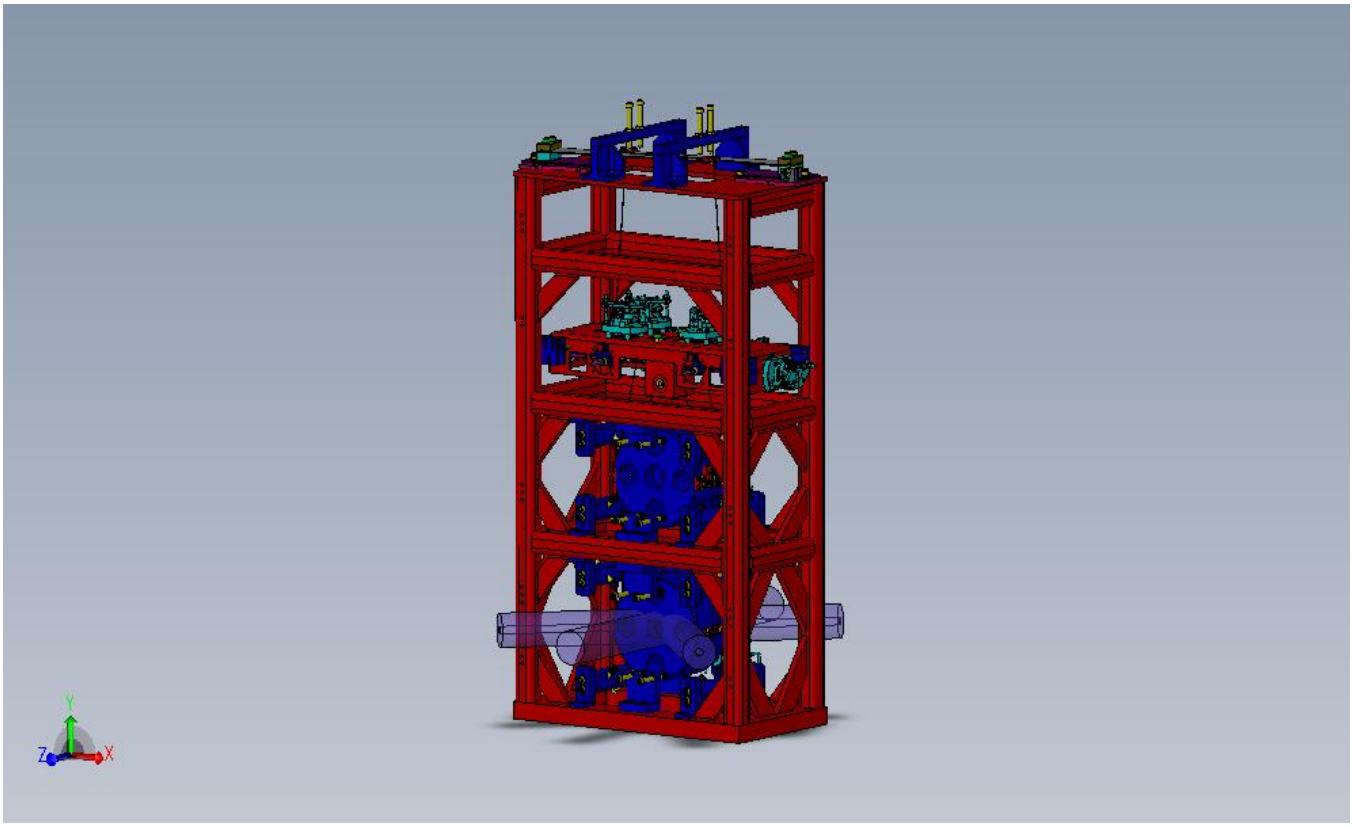

Figure 1. Solidworks rendering of the HAM Small Triple Suspension (HSTS) with a dummy metal mass in place of the optic. The purple beams represent the laser beam entering and reflecting from the optic.

4.2 Blade design

4.2.1 Vertical isolation and stress in blades.

The blade design follows that used in GEO (which was based on the VIRGO design). The blades are approximately trapezoidal and pre-curved so that when the correct load is applied they are flattened. In the designs used in the small triple prototypes already built the blades are conservatively stressed to a level of 600 to 800 MPa, corresponding to the typical stress levels used in the GEO designs. As noted at the preliminary design review we were asked to consider making efforts to increase the vertical isolation. Using the same criteria in the triple blade designs as used for the quadruple pendulums, where a stress level up to ~1 GPa has been used, we can gain a factor of ~ 2 to 4 improvement in isolation. This is more fully discussed in T080267-00-R. The lower blades for the small triple have a proposed thickness of 0.76 mm in this revised design, thinner than we have had manufactured before. In addition the curvature of the blades is much tighter than any blades we have previously had manufactured. Thus we have been going through a further round of prototyping to check that such blades can be made and have the correct characteristics in use. Unfortunately this round of prototyping was not entirely successful. The company was unable to meet the specification on shape and used a procedure (a particular type of press braking) which we

would not have recommended if informed beforehand. At the time of writing we are out for another round of prototyping with two companies to increase our vendor pool and allow us to check whether such highly curved blades can be successfully produced. Thus at this time we cannot confirm what the final design of the blades for the HSTS will be. Since we do not wish to hold up other procurements, on the advice of Dennis Coyne we have chosen to go ahead with the FDR with the proviso that we will need to come back for an update to the FDR when the blade situation is clarified.

4.2.2 Nickel Plating and Production of Blades

The manufacturing specification for all maraging steel blades now includes Ni-plating to mitigate corrosion. A comprehensive process specification for manufacture of all blades for Advanced LIGO has now been produced. See E090023. It includes material requirements, shaping details, detail on the nickel plating process and details of the age hardening fixture. As noted in section 3.2 above, all SUS (US) blades will use maraging 250.

4.3 Structure Design

While a requirement for the resonant frequencies of the HSTS structure has not been formally captured it has previously been understood that the structure should not have a resonant frequency below 150 Hz. This requirement is based on the need for the structure to not compromise the upper unity gain frequency of the HAM-ISI control, which is ~60 Hz. The first prototype structures, made of welded aluminium, predated this requirement and had a first resonance around 50 Hz when loaded with the requisite non-suspended mass, see T030278-05-D. Rework on the design prior to the PDR was captured in T080318-00. Further work since then has yielded a design as shown in Figure 1, which is a stainless steel design with gussets with a calculated first modal frequency from FEA of 121 Hz. More details can be found in T080318-v1.This is a good result given the various restrictions on the design, including the footprint, the mass and the required access. Recently, in discussion with Systems, the emphasis has shifted from the frequency of such structures to their damping, and SUS has been directed to forego further efforts to push up this frequency. We have been asked to add provision for attachment of conceptual stiffening/damping struts to the tops of the HLTS and HSTS structures. This is captured in RODA M080374 (further discussed in section 7.1). This provision has been carried out. At the time of writing Systems and the Stanford research group are carrying out research on the design of suitable struts or other damping methods for suspension structures. In addition Systems have been including conceptual struts in the layout on the HAM tables – see for example D0900465. As and when a design is firmed up we will be ready to accommodate it.

We note that at the time of writing, details of the methods of overall alignment of optics and cavities, details of method(s) of installation of suspensions and details of the routing of electronics cabling have still to be finalised for Advanced LIGO. All of these need holes in the structures and some alignment techniques may require fiducial marks. We have already provided a suite of holes as indicated in figure 2, but are aware that more will be requested. For example we know that holes for attaching parts designed by the IO group to carry out fine alignment of yaw and longitudinal position of the structures on the HAM tables will be required. With regard to this positioning, we have also been asked to call out that the base of the structure should be deburred and that if possible the outer edge be machined to a specific radius.

With regard to the routing of electronic cabling from the OSEMS down the legs of the structure, we note these should be positioned to keep clear of laser beams. Details of the cable positioning will be added to the assembly document when available.

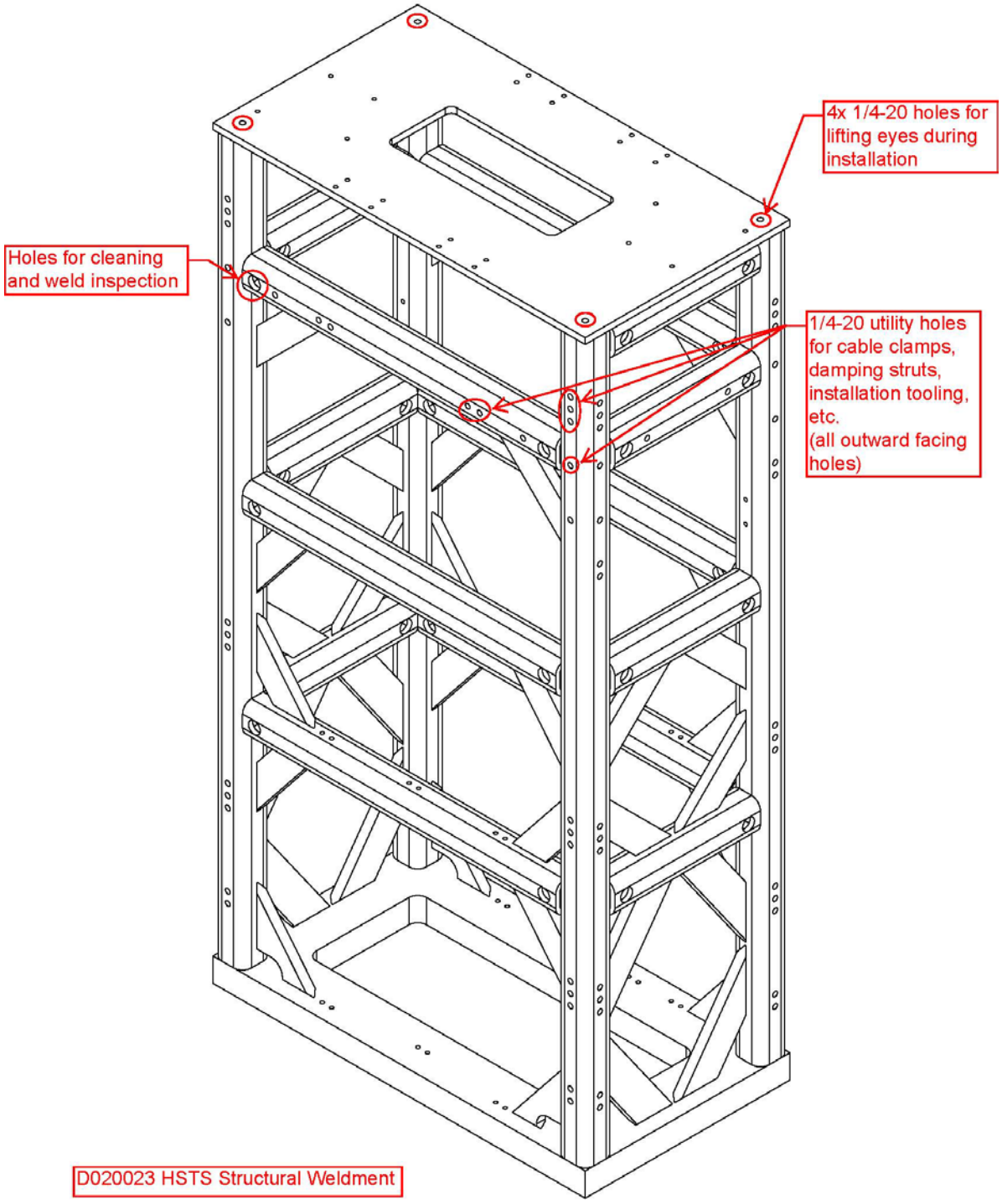

Figure 2. Provision of holes in the HSTS structure

4.4 Final Stage Wire Diameter

At the PDR the question was raised about whether the 28 Hz vertical mode frequency could be pushed down by the use of thinner wires in the final stage. This could in principal lead to a modest improvement in vertical isolation at frequencies above the new peak. The 28 Hz frequency arises from using 60 micron radius wire. This value was set by using a nominal value for tensile strength for music wire of 2000 MPa and using a safety factor of ~3. This has been a guiding principle used in general in our suspension designs. In fact, however, the tensile strength for music wire increases as diameter decreases, and for wire of 60 micron radius (0.12 mm diameter) the minimum tensile strength as per ASTM A-228M-07 is ~2900 MPa (see T0900502). So our safety factor is higher, at least ~4.5. For reference we note that LIGO 1 uses a safety factor of ~ 4.

We could consider using thinner wire if a lower frequency is more desirable. For example a safety factor of 3 over the minimum tensile strength would be achieved with wire of 47.5 micron radius. The frequency of the highest vertical mode would be 22 Hz. If one were willing to use a lower safety factor the frequency could be pushed down correspondingly (with frequency proportional to radius). However to change from the baseline of 60 micron radius is not a simple matter of swapping the wire size. Firstly we would need to design clamps and prisms to accommodate the revised size. The small size is already quite demanding on the manufacturability of these items. One of our vendors for clamps has informed us that we have reached the manufacturing limit on groove size for the current design of grooves. Secondly, we would need to carry out tests of the overall clamp-wire-clamp assembly to check that the clamped wire can sustain the load.

In conclusion, we are not proposing to change the wire radius from the baseline value of 60 micron radius. A request to do so will result in more design work being needed, and possibly prototyping and experimental investigations, depending on the magnitude of the change.

4.5 Prism Design

We have adopted the double prism technique (sapphire prism with laser ablated groove and smaller steel prism below) for suspending the optic, following investigations by Rai Weiss and colleagues on losses in wire suspensions, discussed more fully in section 5 of the preliminary design document T080187. The design is more fully described in T080266-03. We have had some prototype sapphire prisms manufactured (D0810033-v3) and these appear to satisfy our requirements for the HSTS. See figure 3 for an example showing the full prism and the laser ablated groove in profile.

With regard to gluing these prisms in place, we have two possibilities for the sapphire prisms. We could glue them using a vacuum approved glue (replacement for vacseal) following the technique used by Rai Weiss during tests at MIT, which involves using a bead of epoxy around the perimeter of the prism but no epoxy between it and the optic. Alternatively we could use UV cure epoxy between the prism and the optic. One can use a very thin layer of this epoxy. This technique also gives less adhesive area exposed to vacuum. The lower prism can be tacked in place at each end using epoxy. The technique used by Weiss was to insert this prism between the wire and the optic while it was in the wire loop, pushing down until one feels some tension, and then tacking in place. However, if we wished to have ready-bonded optics prepared ahead of installation, we could determine the correct place on an actual suspension and then remove and glue the prism and store the optics till required.

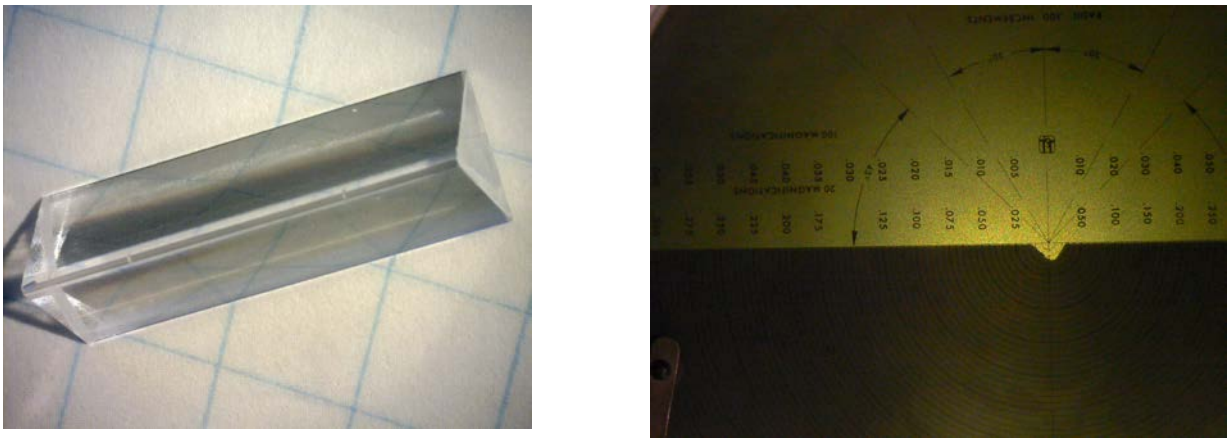

Figure 3. Sapphire prism. Left: whole prism with two grooves just visible on top edge. Right: close up of groove, approximate width and depth = 6 thou.

4.6 Methods of Attaching Magnets

For the bottom two stages of the HSTS, the magnets with standoffs will be glued on, using an approved epoxy. We are using the same shadow geometry for the AOSEMs as was used in initial LIGO, and hence the magnet needs to be at the same sweet spot.

The top magnets are held on magnetically to steel inserts, using the same design as used in the ETM/ITM suspensions.

Renderings of the magnet/standoff arrangement for each stage are shown in figures 4 to 6.

Information on the types and sizes of magnets is given in section 5.

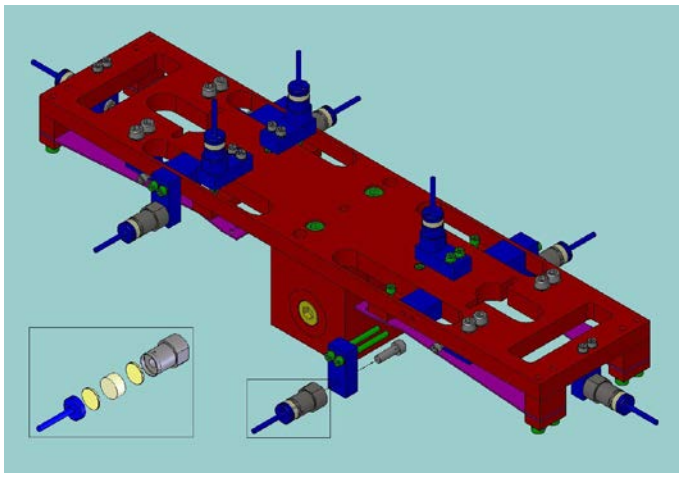

Figure 4. Flag/magnet assembly at top mass

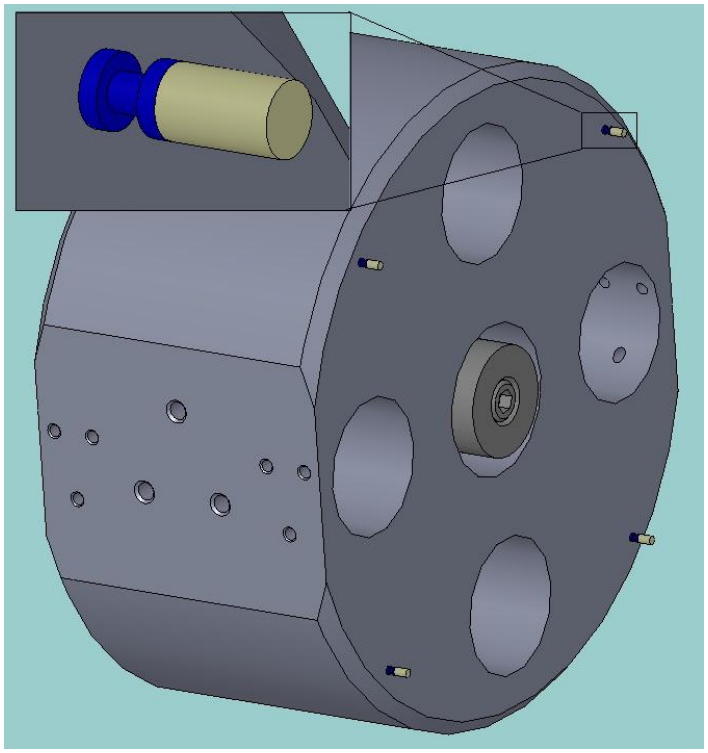

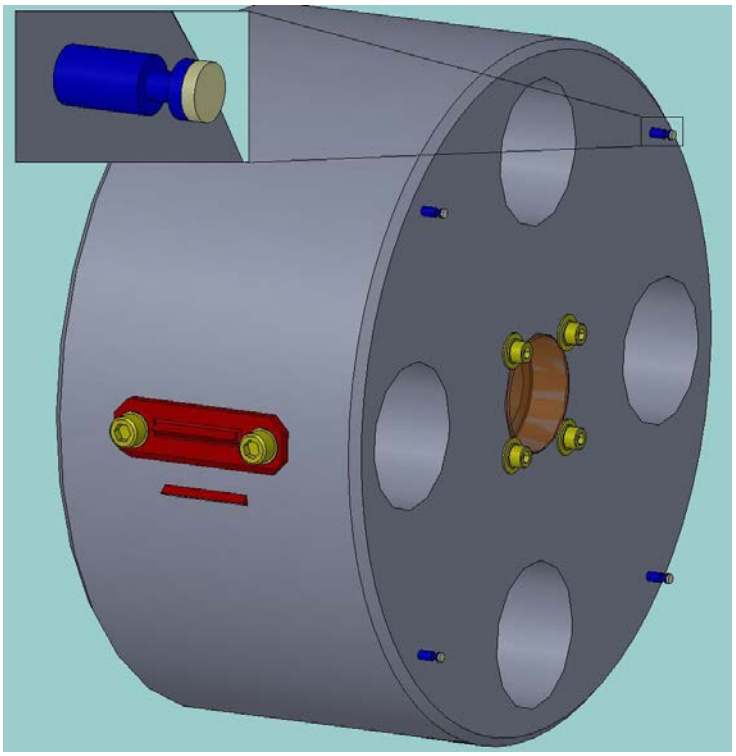

Figure 5 (left). Magnet fixture at middle mass. Figure 6 (right) Magnet fixture at optic (shown on dummy mass)

4.7 Methods for Adjusting Suspension for Different Masses

As noted above, this suspension is used for two different optics, the input modecleaner optics, and the small recycling mirrors PRM, SRM PR2 and SR2. angles and orientation, the input modecleaner has a mass (including attachments) of 2.892 kg and a 0.5 degree wedge, oriented horizontally, and the small recycling mirror optic has a mass of 2.871 kg, and a 1 degree wedge oriented vertically, heavy side down (see E0900342 for wedge information). The nominal mass difference is thus ~ 20 gm. In fact we have been informed by the IO group that due to the tolerances on the diameter and thickness for these optics a wider variation in mass may be expected. In order to arrive at the correct height for the overall suspension, where the static alignment requirement is currently set at +/- 1 mm (see T010007-v2) and to ensure that the tips of the lower blades are close (within 0.5 mm) to the correct height within the top mass, we employ several techniques for adjusting the overall mass and position of the suspension.

Firstly the upper and lower blades have a library of clamps with clamp angle increments of 0.5 degrees, ranging from 0 to +/-3.5^{o} for the upper blades and 0 to +/-2.5^{o} for the lower blades. For reference, the use of a library of clamps for the prototype modecleaner suspensions is discussed in T030125. For the upper blades, of length 25 cm, a 0.5 degree angled clamp changes the tip height by approximately 2 mm. For the lower blades, length 12 cm, a 0.5 degree angled clamp changes the tip height by approximately 1 mm. Thus angled clamps can give fairly large changes, which can be used to correct for variations of stiffness within batches of blades, noting that we will characterise all blades before use and pick matched pairs to minimize asymmetries.

Secondly we can change the masses of the upper and/or middle masses. The upper mass has a 1/4-20 hole on the top and bottom directly in the middle of the mass for adding removable mass. In addition it has provision for moving mass in and out and left and right for trimming pitch and roll respectively. The intermediate mass has a 1/4-20 hole through the center of the mass which is designed so that mass can be added to both sides (front and back) evenly or, if necessary, unevenly to allow the mass to pitch (see assembly drawings D020535, top mass and D0901873, intermediate mass). There are designs for removable mass of 10, 20, 40, 50, and 100 grams. For the baseline design of highly curved blades which we propose to use, the addition of 10 grams will cause a change in deflection of ~ 0.5 mm for both the top and bottom blades.

5 OSEMs, Magnets and DC Control Ranges

The following table is captured from T1300079-v1, where more details and frequency-dependent information can be found. Any future updates to T1300079 supercedes what is captured here.

HAM Small Triple Suspension (HSTS)
Details of OSEMS, Magnets, Coil Drivers and maximum DC drive range at each stage
T1300079-v1
Jeff Kissel
30th January 2013

Max DAC Voltage [V_p]	(Differential voltage across the Plus and Minus legs)
10	

Suspension Stage	OSEM Type	Magnet Type	Magnet Size diameter x thickness	Coil Magnet Actuation Strength	Coil Magnet Actuation Strength
Units	[ ]	[ ]	[mm]	[N/A]	[N/mA]
Top (TOP, M1)	BOSEM	NdFeB	10 x 5	0.963	0.000963
Intermediate Mass (MID, M2)	AOSEM	SmCo	1.905 x 3.175	0.0158	0.0000158
Optic (BOT, M3)	AOSEM	SmCo	2 x 0.5	0.00281	0.00000281

Coil Driver	DC Transconductance	DC Max Current Output	DC Current Range	DC Current Range Requirement	Frequency Range
Units	[mA/V]	[mA_p]	[mA_pp]	[(mA_p) or (mA_rms)]	[Hz]
Triple TOP (D0902747-v4)	11.919	119.19	238.38	60 (p), 200 (rms)	f < 1 Hz, 1 Hz < f < 100
Triple Acq. (D0901047-v4)	0.32635	3.2635	6.527	M2: 3 (p), M3: 0.15 (p)	f < 1 kHz, f < 1 kHz
Modified Triple Acq. (L1200226-v2)	2.8284	28.284	56.568	n/a	n/a

Degree of Freedom (DOF)	Stage	DC Compliance at Mass	Lever Arm	# of OSEMs	DC Compliance at Coil Driver Output	DC Max Disp. from Coil Drive	DC Max Disp. from Coil Drive	DC Disp. Range from Coil Drive	DC Disp. Range from Coil Drive
Units	[ ]	[(m/N) or (rad/N.m)]	[m]	[ ]	[(m/mA) or (rad/mA)]	[(m_p) or (rad_p)]	[(um_p) or (urad_p)]	[(m_pp) or (rad_pp)]	[(mm_pp) or (mrad_pp)]
Longitudinal	M1	0.003405	1	2	6.559E-06	7.817E-04	781.72	1.563E-03	1563.441
Pitch	M1	0.609150	0.03	2	3.520E-05	4.195E-03	4195.09	8.390E-03	8390.186
Yaw	M1	0.426300	0.08	2	6.568E-05	7.829E-03	7828.91	1.566E-02	15657.824
Longitudinal	M2	0.006275	1	4	3.966E-07	1.294E-06	1.29	2.588E-06	2.588
Pitch	M2	2.108700	0.048	4	6.397E-06	2.088E-05	20.88	4.175E-05	41.753
Yaw	M2	1.141500	0.048	4	3.463E-06	1.130E-05	11.30	2.260E-05	22.602
Longitudinal	MODM2	0.006275	1	4	3.966E-07	1.122E-05	11.22	2.243E-05	22.433
Pitch	MODM2	2.108700	0.048	4	6.397E-06	1.809E-04	180.93	3.619E-04	361.863
Yaw	MODM2	1.141500	0.048	4	3.463E-06	9.794E-05	97.94	1.959E-04	195.887
Longitudinal	M3	0.014057	1	4	1.580E-07	5.156E-07	0.52	1.031E-06	1.031
Pitch	M3	2.917500	0.048	4	1.574E-06	5.137E-06	5.14	1.027E-05	10.274
Yaw	M3	2.343800	0.048	4	1.265E-06	4.127E-06	4.13	8.254E-06	8.254

References

DAC Voltage	T1200311-v1		
OSEM and magnet details	M0900034-v4		
OSEM Coil/Magnet Actuation Strengths	T1000164-v3		
DC Compliances for long/pitch/yaw	https://redoubt.ligo-wa.caltech.edu/svn/sus/trunk/Common/MatlabTools/TripleModel_Production/		
	Model:	ssmake3MBf	rev1891
	Parameters:	hstsopt_metal.m	rev2039
	DC compliance ==	Transfer function from given stage drive to test mass; L to L,P to P, and Y to Y	
Coil driver requirements	T060067-v1		
	Informed by	https://awiki.ligo-wa.caltech.edu/aLIGO/TripleSuspensionActuation	
Coil Driver DC Transconductance	https://alog.ligo-la.caltech.edu/aLOG/index.php?callRep=4495		
Lever Arms	D020700-v1		

6 Noise Estimates

A full set of noise estimates (seismic noise, sensor noise, thermal noise, in longitudinal, vertical pitch and yaw degrees of freedom) was prepared for the preliminary design review, see T0810039. Since those graphs were produced, there have been a few changes. Firstly a bug was discovered in the thermal noise code written in Mathematica which was used to derive the thermal noise curves for wire suspensions. This is written up in T0900320. The upside is that the bug caused the thermal noise estimates to be overestimated by a factor of ~ √2 at ~10 Hz and above. Secondly there are minor changes to the suspension parameter file. This has come about due firstly to changes in the wedge angle (and hence also the mass) and orientation for the optics from the value set at the time

of the PDR, and secondly from small changes to some other parameters due to the updating of the design drawings to accommodate required revisions. The current parameter file is given in section 9.

We present in figures 7 and 8 updated noise plots for longitudinal and vertical directions. These have been produced using the optic size and orientation for the HSTS as used in the recycling cavity, where the wedge is 1 degree, asymmetrical and orientation is heavy side down. For reference, the input modecleaner optics have a wedge of 0.5 degrees, asymmetrical oriented horizontally. The requirements are also indicated on the graphs. We again include two versions of the seismic input at the top of the suspension, as supplied by Peter Fritschel and documented in T0810039. The sensor noise curves have been produced in the same way as in T0810039 with active damping using a simple control law. The details of the seismic inputs used and the damping filter are included in sections 11.4 and 11.5 respectively.

We note that the curves are essentially the same as presented in T0810039 except for the ~ √2 improvement in the thermal noise estimates, taking that noise term close to the requirement: at 10 Hz the requirement (with assumptions as presented in section 2) is 1 x 10^{-17} m/√ Hz, whereas the thermal noise is 1.2 x 10^{-17} m/√ Hz. In fact when combined with the thermal noise level of the HLTS, as in eqn 1, the overall thermal noise should be even closer to the requirement since the HLTS noise level is estimated to be lower than the HSTS. Further details will be presented in the HLTS final design review.

Other conclusions are unchanged from those presented in T0810039. There is excess seismic noise in both longitudinal and vertical directions, for longitudinal up to ~ 20 Hz and for vertical up to the 28 Hz peak. We understand that steps are being taken to see if more isolation can be provided by the HAM-ISI. The sensor noise is also high in this 10-20 Hz region. As discussed in T0810039, there are several options to reduce that noise term including using a more aggressive control law, reducing the gain in science mode or using modal damping.

Actuator noise estimates have also now been carried out, specifically for MC2 but should be representative of all HSTS. These can be found in the LLO alog (entries 4490 and 4751) at https://alog.ligo-la.caltech.edu/aLOG/index.php?callRep=4751

7 Final Design Review Checklist

We have taken the checklist given on page 10 of the document M050220-09, "Guidelines for Advanced LIGO Detector Construction Activities" and created an excel spreadsheet E0900262-v1.

For each point on the checklist we have listed on the spreadsheet the document(s) which address that topic (where such exist). We cover below a couple of items not referred to in other documentation.

7.1 Relevant RODAs and ECRs

M060017 "Steel Wires on the Mode Cleaner Suspensions"

M060315-00 "No Flats on Input Mode Cleaner Optic & Recycling Mirror for Advanced LIGO"

M080038-03 "Responsibilities for Elements of the Stable Recycling Cavities"

M080374-00 "HAM Triple Suspensions to have provision for mounting damping struts to the tops of their structures"

M0900034-v3 "Magnet sizes and types and OSEM types in Adv. LIGO suspensions"

M0900087-v1 "All in vacuum cabling will be shielded"

M0900234-v1 "SUS (US) blades will use maraging 250"

M0900271-v1 "Division of Responsibilities for Harnesses for Adv. LIGO Suspensions"

M1000047-v2 "RODA - Decision to modify HAM structures (HLTS, HSTS, OMC)"

M1100117-v2 RODA of HSTS and HLTS stay clear area

M1100192-v1 RODA: Accuracy of height of mirrors in HSTS and HLTS

M1000312-v2 "Use of SS 316 in AOSEMs and BOSEMs".

M1200134-v3 "RODA: Initial SRM Installation Plan"

All of these have been carried out.

In addition there is an ECR (engineering change request) of relevance: **E1201116** "ECR - Replace HSTS Lower Blade Stops". This work has been completed.

7.2 Relevant Risk Registry Items

RR102 "Potential shortage of engineering and skilled touchlabor skills -- solidworks drafters; Conflict with S6 run operators being unavailable"
This risk has been addressed in the development phase with extra staff. We will consider extra staff in project phase if/as needed.

RR 104 "Blade procurement: difficulty in identifying vendor, fabrication process"
This is still an open risk as described in section 4.2.

RR106 "Structure and welding: Vacuum, structural requirements cannot be simultaneously met". Open mitigation actions are " Provide suitable holes in production structures for retrofitting damping struts. Investigate and evaluate effects of struts and other damping mechanisms on test structures". Holes are being provided. The investigations are ongoing by Systems, and any retrofits will be implemented as and when appropriate.

Note that there are a couple of risk items which address electronics. Since it has been decided that we will review triple electronics with the HLTS later this year, these are not addressed here.

Note added in April 2013: these risk registry items are now retired.

7.3 Follow-up design review on assembly.

Since the time of the review for which this document was first prepared, a review was carried out of the assembly procedures for the HSTS and HLTS.ee the report T1100593-v9. A summary of all suspension design reviews, including electronics reviews (carried out separately) is given in T1200463, with details of the follow-ups to close any open items covered in T1200492. In T1200463, items 12, 14, 15, 16, 17, 18, 19 and 22 are all HAM triple suspension related.

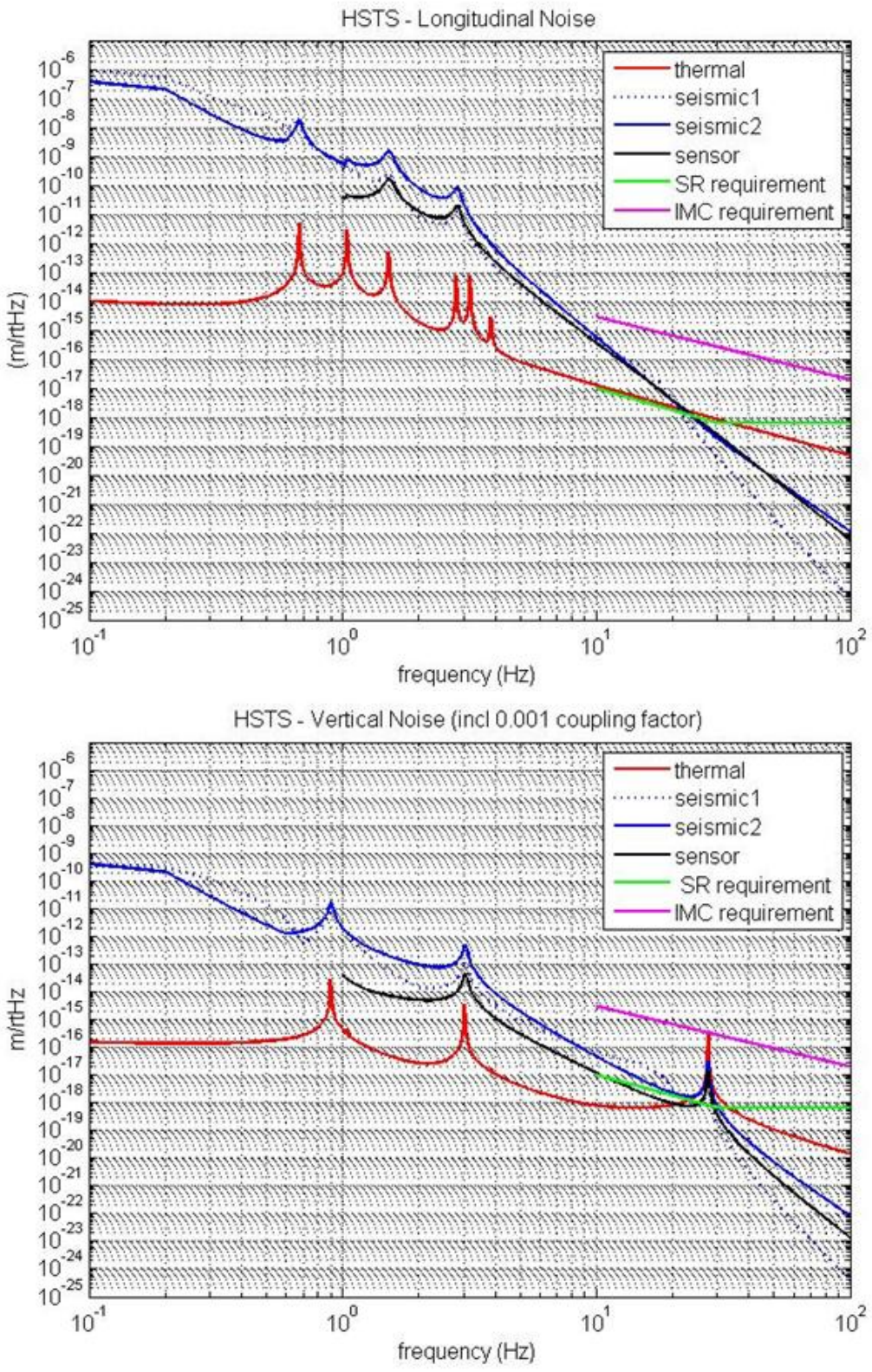

Figures 7 and 8. HSTS noise plots, longitudinal (above), vertical (below). Details as in text.

8 Conclusions

We have presented details of the final design of the HAM Small Triple Suspension (HSTS) which will be used to suspend the input modecleaner optics IMC1, 2, 3 and the small optics within the recycling cavities, PRM, PR2, SRM and SR2. The design builds on the successful design of the modecleaner prototypes built in 2002/2003 and tested at Caltech and subsequently at LASTI where they were used for various investigations. One is still in use for cavity experiments. Since the PDR, we have implemented into the design those items called out in the lessons learned document E080527. We have addressed the requirement to increase the stiffness of the structures, see T080318-v1. We have prototyped the manufacture of sapphire prisms.

As noted at the preliminary design review, there is excess residual seismic noise in both longitudinal and vertical directions at low frequencies, for longitudinal up to ~ 20 Hz and for vertical up to the 28 Hz peak. We understand that steps are being taken to see if more isolation can be provided by the HAM-ISI.

Our design is complete apart from two areas.

8.1 Blades

We have still to demonstrate that thinner highly curved blades can be manufactured satisfactorily. We have recently received two sets of prototypes and will test these shortly. We are also in procurement of a set from a third vendor. We note that the vertical isolation shown in the graphs in figure 4 assume the use of such blades. We will not proceed to procurement of production blades until tests on the prototype blades are completed.

8.2 Structure

We are still to receive input on requirements for holes/fiducial marks for alignment purposes. The topic of alignment is being addressed at a Systems level, and we hope to receive sufficient information fairly shortly to allow us to update the structure drawings before starting the procurement process.

In conclusion, although the above items are still pending, they should be resolved within the next couple of months. We were advised to proceed with the final design review now to allow us to move forward with our schedule for procurement, manufacture and assembly. We are confident that all other aspects are complete and ready for production.

Note added in April 2013: these two outstanding design areas have been completed.

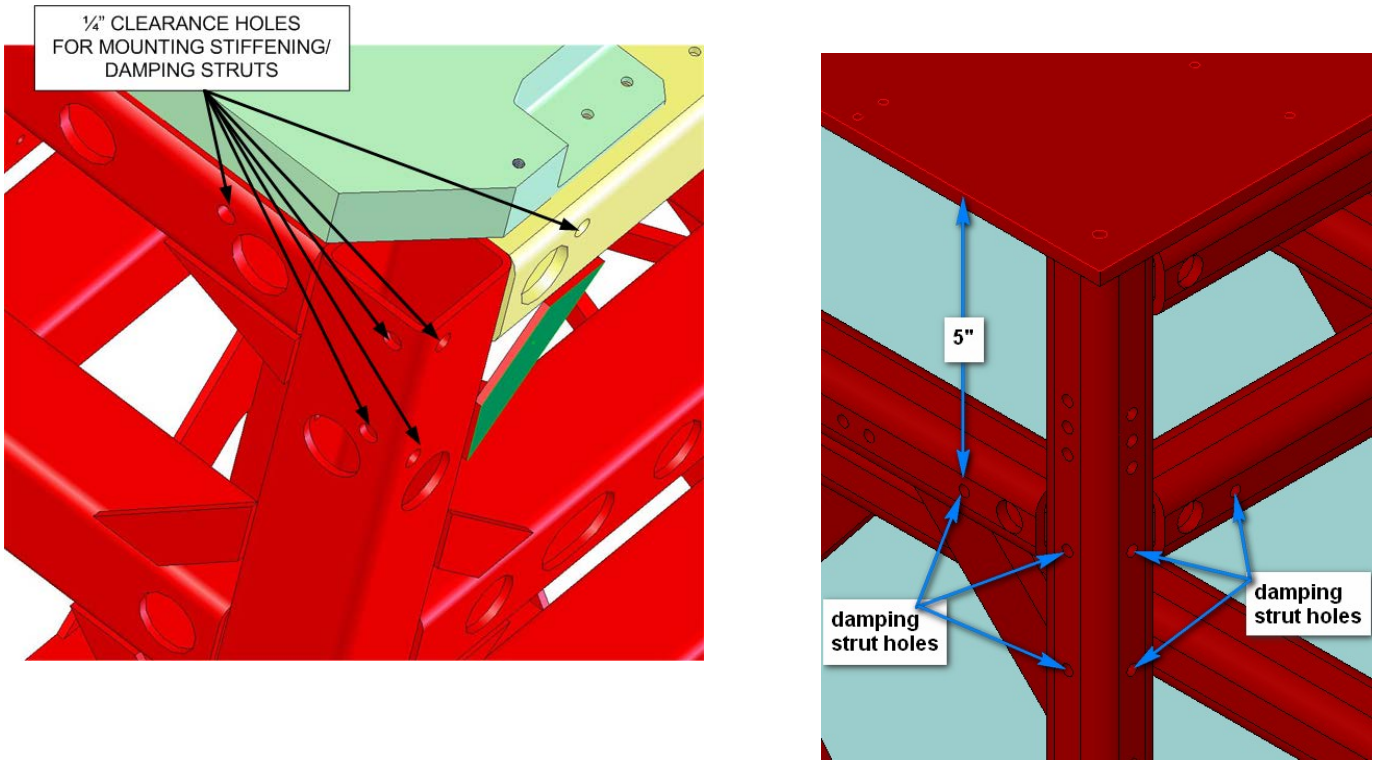

Figure 9. Positions of holes for mounting damping struts, taken from RODA M080374-00 (left), proposed positions of holes for the HSTS (right).

9 Details of MATLAB Model

The MATLAB set of files used to generate the sensor and seismic noise transfer functions used in figures 7 and 8 can be found in T080311–v2. We list below the key parameters and resonant frequencies used in the model. The optic mass (m3) is taken as that for the small recycling mirror with 1 degree vertical wedge and ears and magnets attached. The value of the mass comes from the Solidworks rendering. For the purposes of the MATLAB model, which assumes symmetry, it is modeled as a symmetric right circular cylinder of radius 75 mm and appropriate thickness to give the correct mass. All units are SI. Diagrams and further information explaining the parameter nomenclature are given in sections 11.1 and 11.2.

m1: 3.1276
I1x: 0.0217
I1y: 0.0025
I1z: 0.0216
m2: 2.9686
I2x: 0.0093
I2y: 0.0055
I2z: 0.0064
tx: 0.0738
tr: 0.0750
m3: 2.8706*
I3x: 0.0081
I3y: 0.0053
I3z: 0.0053
l1: 0.2950
l2: 0.1670
l3: 0.2200
nw1: 2
nw2: 4
nw3: 4
r1: 1.8000e-004
r2: 1.0000e-004
r3: 6.0000e-005
Y1: 2.1200e+011

```
    Y2: 2.1200e+011
    Y3: 2.1200e+011
  l1b: 0.2500
  a1b: 0.0399
  h1b: 0.0013
 ufc1: 1.7600
  l2b: 0.1200
  a2b: 0.0180
  h2b: 7.6000e-004
 ufc2: 2.1700
   su: 0
   si: 0.0284
   sl: 0.0050
   n0: 0.0773
   n1: 0.1000
   n2: 0.0390
   n3: 0.0765
   n4: 0.0801
   n5: 0.0800
stage2: 1
   d0: 0.0050
   d1: 0.0020
   d2: 0.0011
   d3: 9.0000e-004
   d4: 1.0000e-003
ribbon: 0
   db: 0
    g: 9.8100
  kc1: 191.2345
  kc2: 275.9313
  tl1: 0.2991
  tl2: 0.1658
  tl3: 0.2219
```

l_suspoint_to_centreofoptic: 0.6869

l_suspoint_to_bottomofoptic: 0.7619

flex1: 0.0020

flex2: 0.0010

flex3: 5.5364e-004

flex3tr: 5.5364e-004

longpitch1: [0.6734 1.0291 1.5149]

longpitch2: [2.7992 3.1658 3.8497]

yaw: [1.1008 2.0507 3.4179]

transroll1: [0.6774 1.5118 1.7118]

transroll2: [2.2647 3.0341 40.5004]

vertical: [0.8985 3.0166 27.5496]

*As seen above, m3 for the recycling mirror is 2.871 kg. For the input modecleaner, which has a smaller 0.5 degree wedge, the mass is 2.892 kg.

10 Details of Mathematica Model

The Mathematica model developed by Mark Barton is described in T020205-02. A web page with further information and examples can be found under the "Triple Pendulum Model Xtra-Lite"at

http://www.ligo.caltech.edu/~e2e/SUSmodels/index.html

The relevant file used to generate the thermal noise curves in figures 3 and 4 is

```
mbtriplelite2_20091016hstsPRM_TN;
```

Further details of the specifications set up for the modeling are given in Section 10.3.

In the Mathematica model the shape of the small recycling mirror with 1 degree vertical asymmetric wedge, thick side down, is fully included in the model (as opposed to being simplified as in the MATLAB model), with mass and moments of inertia as derived from the Solidworks rendering. Thermal noise curves were also generated for the input modecleaner optic (0.5 degree horizontal wedge). In practice the curves are almost identical, and so have not been included here.

The resonant frequencies (in Hz), derived from the Mathematica model, are given below. Very good agreement (generally to at least 3 significant figures) is found between these frequencies and those derived in the MATLAB model presented in section 8. The only mode which differs in the third significant figure (difference of ~ 1%) is the first pitch mode (mode 4 below), influenced by the vertical wedge which is fully modeled in Mathematica but not in the simpler MATLAB code.

```
N   f   type*
1   0.6732675936543286  x3  x2
2   0.6772252162457628  y3  y2
3   0.8985205820938204  z2  z3
4   1.042391847299986   pitch3
5   1.1006145566867878  yaw3    yaw2    yaw1
6   1.5120837584229099  y2  y1  y3
7   1.5148563223768725  x2  x1  x3
8   1.7158185008442466  roll2   roll3
9   2.0505602976453488  yaw1    yaw3
10  2.2650310649330314  roll1
11  2.7992087123698095  x1  x2
12  3.0165568681350563  z1
13  3.0340518590627013  y1  y2
14  3.169619288577941   pitch1  pitch3
15  3.4178322607283933  yaw2    yaw3
16  3.8505972023054436  pitch1  pitch2
17  27.549200288160325  z3  z2
18  40.50988696026382   roll3
```

* Note that the coordinates (“type”) in the listing come from a crude mode ID function that ranks the coefficients in the eigenvector in descending order and prints coefficient names until half the total squared amplitude in the mode has been accounted for.

11 Appendices

11.1 Diagrams Showing Triple Pendulum Parameters

The parameters for a triple pendulum (face on view).

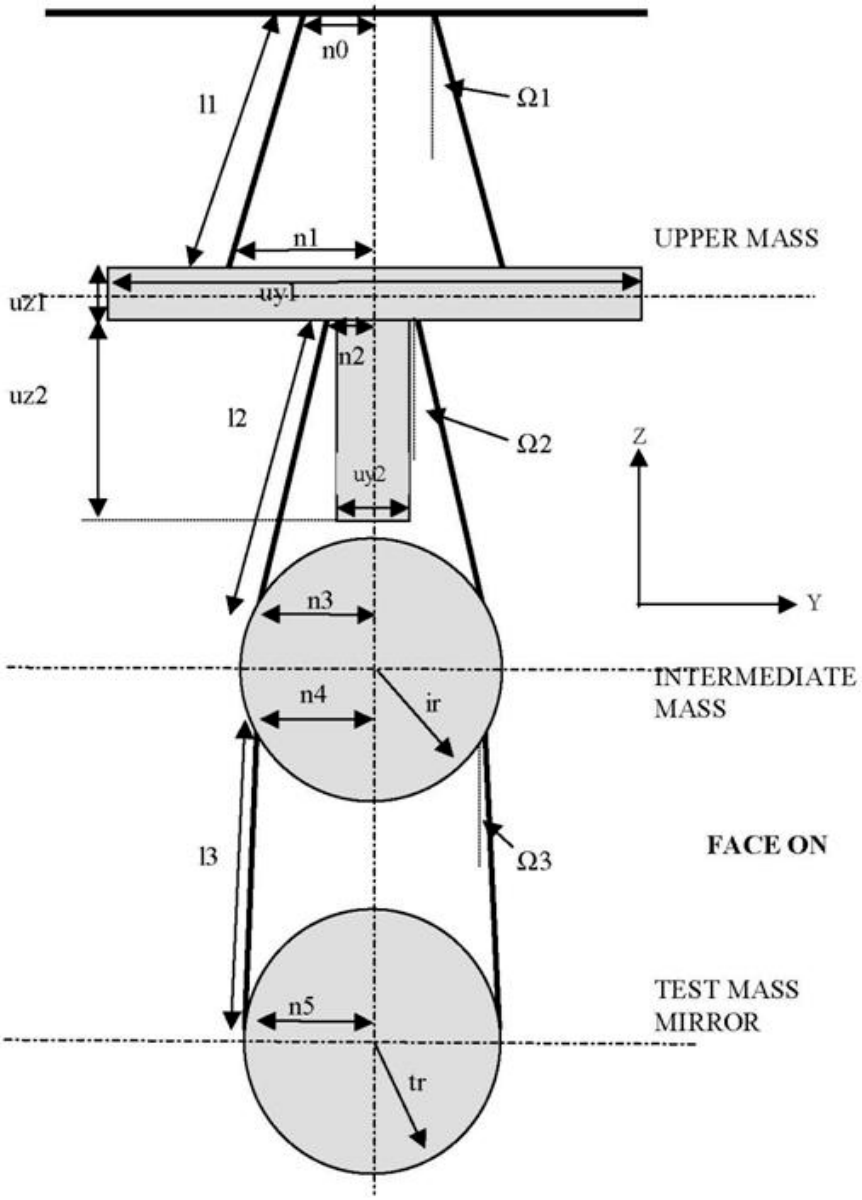

The parameters of a triple pendulum (side view).

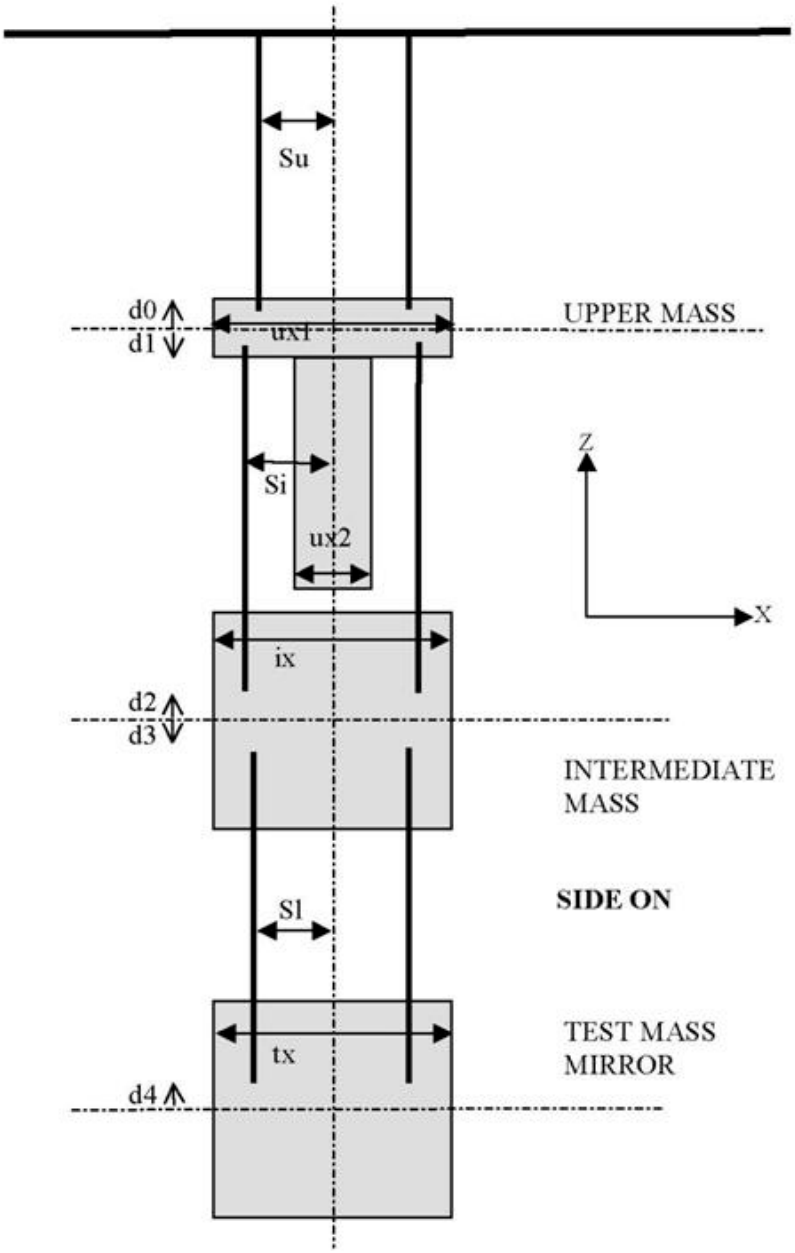

11.2 Explanation of parameters listed in section 9 (other than those shown in the diagrams above).

m1, m2, m3: masses from top to bottom

Iix, Iiy, Iiz where i = 1,2,3 from top to bottom mass = moments of inertia as follows
Iix: moment of inertia (transverse roll)
Iiy: moment of inertia (longitudinal pitch)
Iiz: moment of inertia (yaw)

nwi = number of suspension wires at each stage from top to bottom

ri = wire radius from top to bottom

Yi = Young's modulus of wire/fibre from top to bottom

l1b, a1b, h1b: length, width at root, thickness of top blades

ufc1: uncoupled frequency of top blade with mass immediately below it

l2b etc – same as above for lower blades

stage 2 = 1
If pend.stage2 is defined and non-zero, d0-d4 are interpreted as raw values, i.e., as actual wire breakoff vertical positions

tl1, tl2, tl3: centre to centre vertical separations at each stage - from top suspension point to centre of top mass, centre of top mass to centre of intermediate mass, and centre of intermediate mass to centre of beamsplitter optic respectively

ribbon = 0: round wires/fibres are used (i.e not ribbons)

db = 0: no natural damping included

g: accel. due to gravity

kc1, kc2: blade stiffness (top and bottom respectively)

l_suspoint_to_centreofoptic: length from top suspension point to centre of topic = tl1+tl2+tl3

l_suspoint_to_bottomofoptic: length from top suspension point to bottom of optic

flex1, flex2, flex3: flexure length for wire (top to bottom respectively)

flextr – flexure length for ribbon in transverse/roll direction (same as flex3 if round fibre used)

11.3 Further specifications used in the Mathematica model

```
 modelcase = "20091016hstsPRM";

modelcasecomment = "Norna's HSTS parameter set of 10/13/09 plus PRM optic data of 10/16 from
Mike";

overrides = {
      lockedblades->False, (* False for maximum realism. True for 100% Matlab compatibility *)
      kw1usual -> (Y1*A1)/l1,
      kw2usual -> (Y2*A2)/l2,
      kw3usual -> (Y3*A3)/l3,
      kbuzusual -> (m1/2)*(2*N[Pi]*ufc1)^2,
      kblzusual -> (m2/4)*(2*N[Pi]*ufc2)^2,
      kw1 -> If[lockedblades,recipadd[kw1usual, kbuzusual],kw1usual],
      kw2 -> If[lockedblades,recipadd[kw2usual, kblzusual],kw2usual],
      kw3 -> kw3usual,
      kbuz -> If[lockedblades,10^4*kbuzusual,kbuzusual],
      kblz -> If[lockedblades,10^4*kblzusual,kblzusual],
      kbuy -> If[lockedblades,10^4*kbuzusual,10^4*kbuzusual],
      kbly -> If[lockedblades,10^4*kblzusual,10^4*kblzusual],
      kbux -> If[lockedblades,10^4*kbuzusual,10^2*kbuzusual],
      kblx -> If[lockedblades,10^4*kblzusual,10^2*kblzusual],
      mbeu->0 (*If[lockedblades, 0.005/10^5, 0.005]*),
      mbel->0 (*If[lockedblades, 0.005/10^5, 0.005]*),

      den1->4000,
      ux->0.06, (* display only *)
      uy->0.44, (* display only *)
      uz->0.142, (* display only *)
      I1x ->0.0217, (* Mike Meyer SW model October 8th 2009 *)
      I1y ->0.0025, (* Mike Meyer SW model October 8th 2009 *)
      I1z ->0.0216, (* Mike Meyer SW model October 8th 2009 *)
      m1 ->3.1276, (* Mike Meyer SW model October 8th 2009 *)


      den2->2202,
      ix->0.075, (* display only *)
      ir->0.075, (* display only *)
      m2->2.9686, (* Mike Meyer SW model October 8th 2009 *)
      I2x->0.0093, (* Mike Meyer SW model October 8th 2009 *)
      I2y->0.0055, (* Mike Meyer SW model October 8th 2009 *)
      I2z->0.0064, (* Mike Meyer SW model October 8th 2009 *)
      COM2y->-COM3y,
      I2xy->-I3xy,
```

```
wedge->1*Pi/180, (* D0901172-v4 *)
tx->0.075-tr*wedge, (* display only *))
tr->0.075,
den3->2202,
m3->2.87073885, (* Mike Meyer SW model October 16th 2009 *)
I3x->0.00806676, (* Mike Meyer SW model October 16th 2009 *)
I3y->0.00532667, (* Mike Meyer SW model October 16th 2009 *)
I3z->0.00534182, (* Mike Meyer SW model October 16th 2009 *)
I3zx->0.00003436, (* Mike Meyer SW model October 16th 2009 *)
I3xy->0, (* Mike Meyer SW model October 16th 2009 *)
I3yz->0, (* Mike Meyer SW model October 16th 2009 *)
COM3x->0.00070502,
COM3y->0,
COM3z->-0.00033435,
FRP3x->COM3x, (* both prisms are glued on the same amount forward *)

l1->0.445-0.15,
l2->0.287-0.12,
l3->0.28-0.06,
dl -> COM3y*m3*g/kw3/n5/4, (* correction to wire length to offset wedge mass imbalance *)

r1->180. 10^-6, (* ?? *)
r2->100. 10^-6,    (* ?? *)
r3->60. 10^-6,  (* radius of lower wire, possible new value using steel, July 05 *)

bssteel -> 2*10^9, (* breaking stress of steel *)
wssilica -> 7.7*10^8, (* working stress of silica *)
r1opt->Sqrt[3*(m1+m2+m3)*g/nw1/c1/bssteel/N[Pi]],
r2opt->Sqrt[3*(m2+m3)*g/nw2/c2/bssteel/N[Pi]],
r3opt->Sqrt[(m3)*g/nw3/c3/wssilica/N[Pi]],

Y1->Ysteel,
Y2->Ysteel,
Y3->Ysteel,

ufc1->1.76, (* Norna's bladespec_MC_not-higher_stress_Oct_12_2009.xls *)
ufc2->2.17, (* Norna's bladespec_MC_not-higher_stress_Oct_12_2009.xls *)

d0->0.005, (* Mike Meyer SW model October 8th 2009 *)
d1->0.002,  (* Mike Meyer SW model October 8th 2009 *)
d2->0.0011, (* Mike Meyer SW model October 8th 2009; had been 0.001 *)
d3->0.0009, (* Mike Meyer SW model October 8th 2009; had been 0.001 *)
d4->0.001, (* Mike Meyer SW model October 8th 2009 *)

su->0,
```

```
si->0.0284, (* Mike Meyer SW model October 8th 2009 *)
sl->0.005,

n0->0.0773,          (* MEASURED IN SW 25 SEPT 2003 CIT *)
n1->0.100,
n2->0.039,           (* MEASURED IN SW 25 SEPT 2003 CIT *)
n3->ir-0.0035+0.005,
n4->0.0801, (* Mike Meyer SW model October 8th 2009 *)
n5->0.0800, (* Mike Meyer SW model October 8th 2009; note not equal n4 *)

flex1 -> Sqrt[nw1 M11 Y1/(m1+m2+m3)/g]*c1^(3/2),
flex2 -> Sqrt[nw2 M21 Y2/(m2+m3)/g]*c2^(3/2),
flex3 -> Sqrt[nw3 M31 Y3/m3/g]*c3^(3/2),

rhosilica -> 2.2 10^3, (* gwinc/IFOModel v1.0 *)
Csilica -> 772., (* gwinc/IFOModel v1.0 *)
Ksilica -> 1.38,  (* gwinc/IFOModel v1.0 *)
alphasilica -> 3.9 10^-7, (* measurements by PW, AH - cf. 5.1 10^-7 from gwinc *)
betasilica -> 1.52 10^-4, (* gwinc/IFOModel v1.0 *)
Ysilica -> 7.2*10^10, (* spec sheet for silica *)
phisilica -> 4.1 10^-10, (* gwinc/IFOModel v1.0 *)
phissilica -> 3. 10^-11, (* Phil Willems *)
dssilica -> 1.5 10^-2, (* gwinc/IFOModel v1.0 *)

rhosteel-> 7800., (* gwinc/IFOModel v1.0 *)
Csteel-> 486., (* gwinc/IFOModel v1.0 *)
Ksteel-> 49., (* gwinc/IFOModel v1.0 *)
alphasteel-> 12. 10^-6, (* gwinc/IFOModel v1.0 *)
betasteel-> -2.5 10^-4, (* gwinc/IFOModel v1.0 *)
phisteel-> 2. 10^-4, (* gwinc/IFOModel v1.0 = Geppo's value  *)
Ysteel -> 2.12 10^+11, (* measured by MB, 11/18/05 *)

rhomarag-> 7800., (* gwinc/IFOModel v1.0 *)
Cmarag-> 460., (* gwinc/IFOModel v1.0 *)
Kmarag-> 20., (* gwinc/IFOModel v1.0 *)
alphamarag-> 11. 10^-6, (* gwinc/IFOModel v1.0 *)
betamarag-> -2.5 10^-4, (* Geppo's value - gwinc/IFOModel v1.0 is wrong *)
phimarag-> 1. 10^-4, (* gwinc/IFOModel v1.0 *)
Ymarag-> 1.87 10^11, (* gwinc/IFOModel v1.0 *)

(* Zener, 1938, Phys. Rev. 53:90-99 *)
magicnumber->1/4/FindRoot[0==D[BesselJ[1,x],x],{x,1.8}][[1,2]]^2,

tmU-> 0.0025, (* upper blade thickness, NAR 8/4/06 *)
tmL-> 0.0017, (* lower blade thickness, NAR 8/4/06 *)
```

```
      deltabladeU->Ymarag*alphamarag^2*temperature/(rhomarag*Cmarag), (* cf Bench delta_v1
*)
      deltabladeL->Ymarag*alphamarag^2*temperature/(rhomarag*Cmarag), (* cf Bench delta_v3
*)
      deltawireU->Ysteel*temperature*(alphasteel-
betasteel*g*(m1+m2+m3)/(nw1*N[Pi]*r1^2*Ysteel))^2/
            (rhosteel*Csteel), (* cf Bench delta_h1 *)
      deltawireL->Ysteel*temperature*(alphasteel-
betasteel*g*(m2+m3)/(nw2*N[Pi]*r2^2*Ysteel))^2
            /(rhosteel*Csteel), (* cf Bench delta_h3 *)
      deltafibre->Ysteel*temperature*(alphasteel-betasteel*g*(m3)/(nw3*N[Pi]*r3^2*Ysteel))^2
            /(rhosteel*Csteel),

      taubladeU->rhomarag*Cmarag*tmU^2/(Kmarag*N[Pi]^2),
      taubladeL->rhomarag*Cmarag*tmL^2/(Kmarag*N[Pi]^2),
      tauwireU->magicnumber*rhosteel*Csteel*(2*r1)^2/Ksteel, (* cf Bench tau_steel1 *)
      tauwireL->magicnumber*rhosteel*Csteel*(2*r2)^2/Ksteel, (* cf Bench tau_steel3 *)
      taufibre->magicnumber*rhosteel*Csteel*(2*r3)^2/Ksteel,

      damping[imag,bladeUtype] -> ((phimarag +
deltabladeU*(2*N[Pi]*#1*taubladeU)/(1+(2*N[Pi]*#1*taubladeU)^2))&),
      damping[imag,bladeLtype] -> ((phimarag +
deltabladeL*(2*N[Pi]*#1*taubladeL)/(1+(2*N[Pi]*#1*taubladeL)^2))&),
      damping[imag,wireUtype] -> (phisteel&),
      damping[imag,wireLtype] -> (phisteel&),
      damping[imag,wireUatype] -> ((phisteel +
deltawireU*(2*N[Pi]*#1*tauwireU)/(1+(2*N[Pi]*#1*tauwireU)^2))&),
      damping[imag,wireLatype] -> ((phisteel +
deltawireL*(2*N[Pi]*#1*tauwireL)/(1+(2*N[Pi]*#1*tauwireL)^2))&),
      damping[imag,fibretype] -> ((phisteel)&),
      damping[imag,fibreatype] -> (
            (phisteel + deltafibre*(2*N[Pi]*#1*taufibre)/(1+(2*N[Pi]*#1*taufibre)^2))&
```

11.4 Seismic input for noise curves

seisHAM.m (supplied by Peter F)

```
% [ampX, ampZ, ampRX, ampRZ, ampSP] = seisHAM(f)
%   displacement amplitude spectrum of HAM ISI table
%
% based on data from
% http://ilog.ligo-
wa.caltech.edu/ilog/pub/ilog.cgi?group=detector&date_to_view=
% 07/17/2008&anchor_to_scroll_to=2008:07:18:07:34:50-blantz
% and the proposed HAM HEPI X-beam modification (see HAM ISI PDR)
%
% note that ampY and ampRY are assumed to be equal to ampX and ampRX
% ampSP is the suspension point motion for the targeted HAM ISI requirement

function [ampX, ampZ, ampRX, ampRZ, ampSP] = seisHAM(f)

  % frequency, ampX, ampZ, ampRX, ampRZ
  fa = [1e-3 1e-6 1e-6 1e-7 1e-7
    0.1 1e-6 4e-7 4e-8 3e-7
    0.2 5e-7 3e-7 2e-8 4e-8
    0.3 1e-7 1e-7 5e-9 1e-8
    0.4 3e-8 3e-8 3e-9 4e-9
    0.5 1e-8 1e-8 1e-9 2e-9
    0.6 2e-9 2e-9 8e-10 8e-10
    0.7 4e-10 2e-10 8e-11 1e-10
    0.8 5e-10 3e-10 1e-10 2e-10
    1.0 3e-10 4e-10 8e-11 1.5e-10
    1.4 6e-11 1e-10 1.5e-11 4e-11
    2 2e-11 3e-11 1e-11 3e-11
    5 2.2e-11 4e-11 7e-12 2e-11
    10 3e-11 6e-11 3e-12 4e-12
    13 4e-11 8e-11 4e-12 2e-12
    15 5e-11 1e-10 6e-12 1.5e-12
    18 4e-11 6e-11 4e-12 1e-12
    24 7e-12 8e-12 1.5e-12 6e-13
    30 3e-12 3e-12 1e-12 3e-13
    60 3e-13 3e-13 1.5e-13 8e-14
    100 6e-14 6e-14 3e-14 2e-14
    1e3 1e-14 1e-14 1e-14 1e-14
    1e4 1e-15 1e-15 1e-15 1e-15];

  ampX = exp(interp1(log(fa(:,1)), log(fa(:,2)), log(f), 'cubic'));
  ampZ = exp(interp1(log(fa(:,1)), log(fa(:,3)), log(f), 'cubic'));
  ampRX = exp(interp1(log(fa(:,1)), log(fa(:,4)), log(f), 'cubic'));
  ampRZ = exp(interp1(log(fa(:,1)), log(fa(:,5)), log(f), 'cubic'));

  % proposed requirement displacement noise
  % frequency, ampSP (Suspension Point)

  faSP = [1e-2 4e-6
      0.1 4e-7
      0.2 2e-7
```

```
      0.6 6.66e-10
      1.0 4.0e-10
      10 4.0e-11
      30 1.33e-11
      100 1.33e-11];

  ampSP = exp(interp1(log(faSP(:,1)), log(faSP(:,2)), log(f), 'cubic'));
```

11.5 Control Law used for Damping

GEO active filter design as used in MATLAB model:

Consists of a lowpass, a high pass and two transitional differentiators as follows

lowpass(fcut,dcGain) with values (9, 1)

highpass(fcut,hfGain) with values (0.7,1)

transdif(lf,hf,dcGain) with values (0.35,0.7,1) and (1,9,1)

where the functions are

lowpass
z = [];
p = -2*pi*fcut;
k = dcGain*2*pi*fcut;

highpass
z = 0;
p = -2*pi*fcut;
k = hfGain;

transdif
z = -2*pi*lf;
p = -2*pi*hf;
k = dcGain*(hf/lf);

Bode diagram shown below.

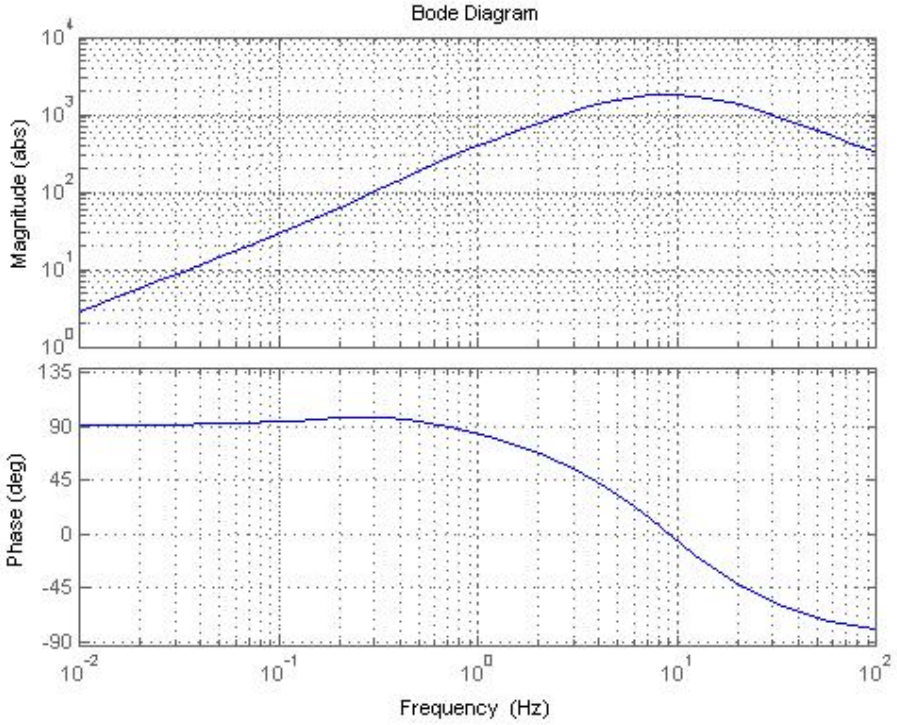
Bode Diagram
Magnitude (abs)
Phase (deg)
Frequency (Hz)
10^4
10^3
10^2
10^1
10^0
135
90
45
0
-45
-90
10^-2
10^-1
10^0
10^1
10^2